CONF-75-187-E
E-0311
C75/05/02
#311

(To appear in the Proceedings of the IV International Nucleon-Antinucleon Symposium, Syracuse University, May, 1975)

Charged-Particle Multiplicities in 100 GeV/c $\bar{p}p$ Interactions

J. Whitmore, W. Morris, B. Y. Oh, D. L. Parker, G. A. Smith
Michigan State University, E. Lansing, Michigan 48824, USA*

R. E. Ansorge, C. P. Bust, J. R. Carter, A. N. Graham,
W. W. Neale and J. G. Rushbrooke
Cavendish Laboratory, Cambridge, England**

C. Moore, R. Raja, L. Voyvodic and R. L. Walker
Fermi National Accelerator Laboratory, Batavia, Ill.,60510,USA†

ABSTRACT

Preliminary results are presented on the topological cross sections produced in antiproton-proton interactions from an exposure of the Fermilab 30-inch bubble chamber to a 100 GeV/c enriched $\bar{p}$ beam. The $\bar{p}p$ inelastic cross section is determined to be $\sigma_{inel} = 34.65 \pm 0.23$ mb, and the average inelastic charged particle multiplicity is $\langle n_c \rangle = 6.74 \pm 0.11$.

In this paper we present some preliminary results of an investigation of antiproton-proton interactions at 100 GeV/c. From a 98,000 picture exposure of the Fermilab 30-inch hydrogen bubble chamber-wide gap spark chamber hybrid system to an enriched $\bar{p}$ beam, we have measured the elastic and the inelastic topological cross sections in 100 GeV/c $\bar{p}p$ interactions. These data comprise the first detailed study of the $\bar{p}p$ collision process at an incident beam momentum above 32 GeV/c.

The enriched beam used in this experiment was obtained from 300 GeV/c primary protons incident on a target 1000 m upstream of the Fermilab 30-inch bubble chamber. Since a negatively charged 100 GeV/c secondary particle beam contains only ~0.02 $\bar{p}/\pi^-$, we used the following technique[1] to achieve a higher $\bar{p}/\pi^-$ ratio: downstream of the target a bending magnet swept out a majority of the secondary charged particles. Following a decay region we then select a

100 GeV/c negative beam. With appropriate tuning of the production angle to preferentially select $\bar{p}$'s produced by $\bar{\Lambda}^{\circ}$ decay over π^-'s from K° decay we obtained a beam with 0.20 $\bar{p}$'s/negative particle. With the further requirement of either (a) more than 1 $\bar{p}$/pulse or (b) a deflection trigger on a tagged $\bar{p}$ beam particle before exposing the bubble chamber, we obtained 98,000 pictures containing an average of 0.32 $\bar{p}$'s/negative particle.

The results presented here come from a sample of ~30,000 pictures which were scanned for all interactions. After an event is found in the bubble chamber, a three-view measurement of the interacting beam track permitted a comparison between the spatial position of that track and the position reconstructed from upstream multiwire proportional chambers[2] (MWPC) in time coincidence with a 35 m long differential gas Cerenkov counter located 500 m upstream from the bubble chamber. This correlation between a reconstructed bubble chamber track and a Cerenkov tagged trajectory in the MWPC was possible for ~85% of the events. The remaining 15% represent only a loss of data[2] and do not bias the data in any way. For the remainder of this paper we use only those events which have a positive $\bar{p}$ identification. By measuring the counting rates in the two segments of the Cerenkov counter as a function of the helium gas pressure, we estimate that when the pressure was set so that the $\bar{p}$'s were below threshold (for ~2/3 of the run), the background in the $\bar{p}$ signal due to inefficiencies in the system are below 2% and have been ignored. About 1/3 of the data were taken with a positive $\bar{p}$ signal and the inefficiency in this mode is below 1%. The data taken in the two modes are in excellent agreement and have been combined.

A small number of frames (~10%) have been rescanned in order to determine the scanning efficiency for various topologies. The resulting efficiencies range from about 92% for 2 prongs to about 99% for 8 prongs and up. All events ($\lesssim$0.5%) with an apparent odd number of charged particles have been classified as belonging to the next highest even charged particle topology. Corrections have been made for unobserved π° Dalitz decays. No correction has been deemed necessary for charged secondary interactions which might occur close to the primary vertex since those tend to populate the odd topologies.

The major correction applied to the raw data occurs for the two prong topology. All two prong events have been measured and a kinematic fit to the $\bar{p}p$ elastic scattering hypothesis has been attempted. Following a preliminary study of the elastic fits, we have corrected the elastic t distribution (t is the square of the four-momentum transfer from target to outgoing proton) by fitting the data (see Fig. 1a) to an exponential form $\frac{d\sigma}{dt} = Ae^{bt}$. We find slope parameters of $b = 10.8 \pm 0.6$ (5.2 ± 0.4) $(GeV/c)^{-2}$ for 100 GeV/c $\bar{p}p$ elastic (inelastic) scattering. We note that no small t correction to the inelastic two prong cross section is necessary (Fig. 1b). We note that the slope of the elastic t distribution is consistent with an extrapolation from lower energies (Fig. 2), and is in good agreement with the result from a counter experiment at 100 GeV/c (Ref. 3).

In Table I we present our measured topological cross sections for 100 GeV/c $\bar{p}p$ interactions. These cross sections have been normalized to the counter data on total cross sections.[4] For comparison, we also give in Table I the 102 GeV/c pp cross sections determined in a previous experiment.[5] Our $\bar{p}p$ elastic cross section of $\sigma_{el} = 7.39 \pm 0.31$ mb would appear to be in good agreement with an extrapolation from lower energies (see Fig. 3).

In Figure 4 we show the variation of the $\bar{p}p$ topological cross sections with increasing beam momentum. The general features of this plot are similar to those observed, for example, in π^-p collisions. In particular, we observe that the 0-prong cross section is falling rapidly and may be parametrized as $\sigma_0(mb) = 62.7\ P_{lab}(GeV/c)^{-1.48}$ between $P_{lab} = 15$ and 100 GeV/c. The 2, 4, and 6-prong cross sections are falling at 100 GeV/c while the cross sections for producing 8 or more charged particles are still increasing at 100 GeV/c.

From the inelastic cross sections given in Table I, we compute various moments of the $\bar{p}p$ multiplicity distribution (see Table II). We determine an average charged particle multiplicity of $\langle n_c \rangle = 6.74 \pm 0.11$. In Figure 5 we show $\langle n_c \rangle$ as a function of the center of mass energy, $\sqrt{s}$, for $\bar{p}p$ interactions. It is interesting to compare the $\bar{p}p$

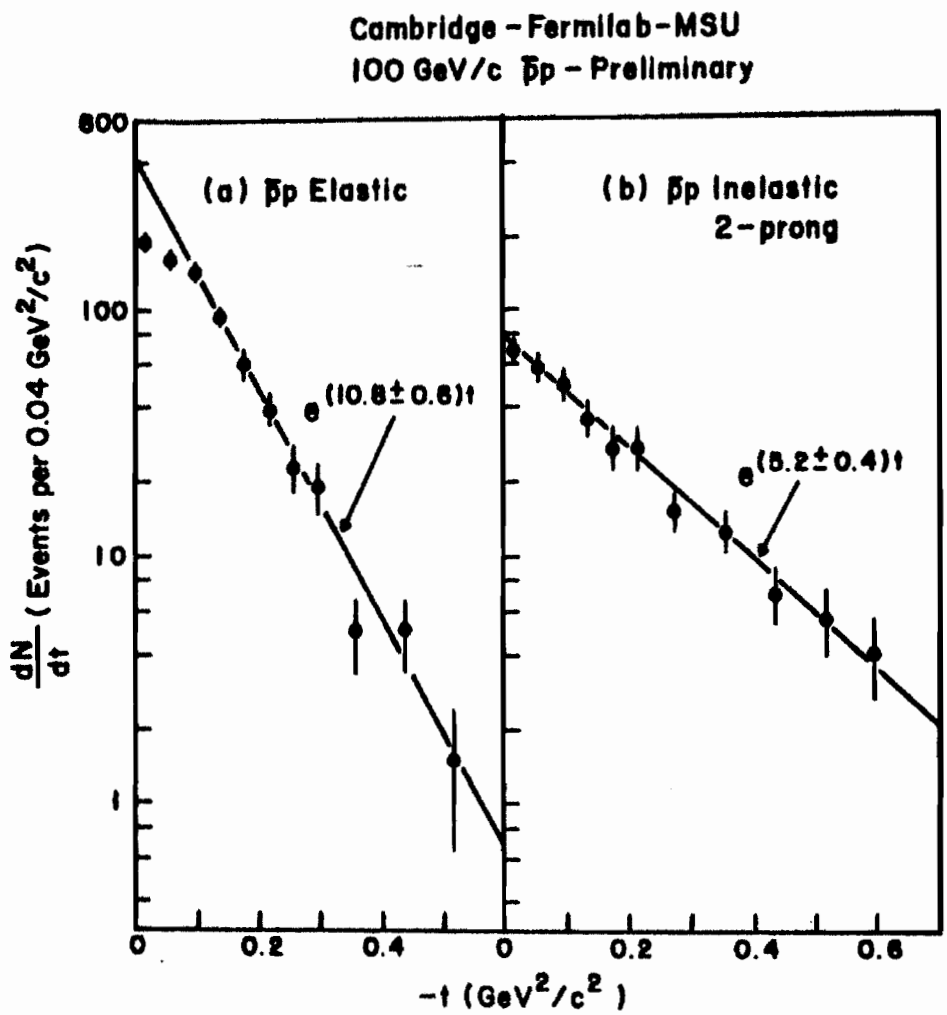

Fig. 1. t distributions for 100 GeV/c $\bar{p}p$ interactions: (a) elastic scattering, and (b) 2 prong inelastic scattering.

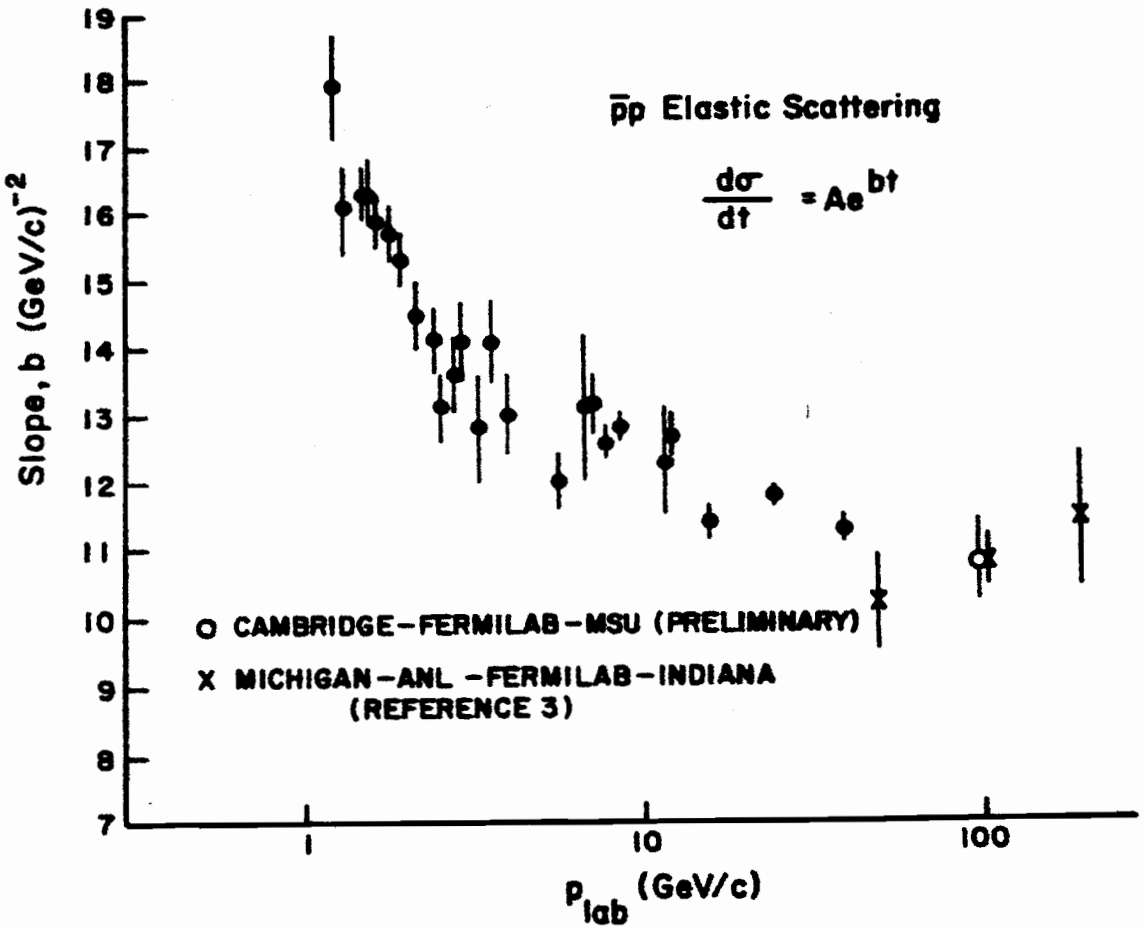

Fig. 2. Slope of the p̄p elastic scattering t distribution as a function of the incident p̄ momentum.

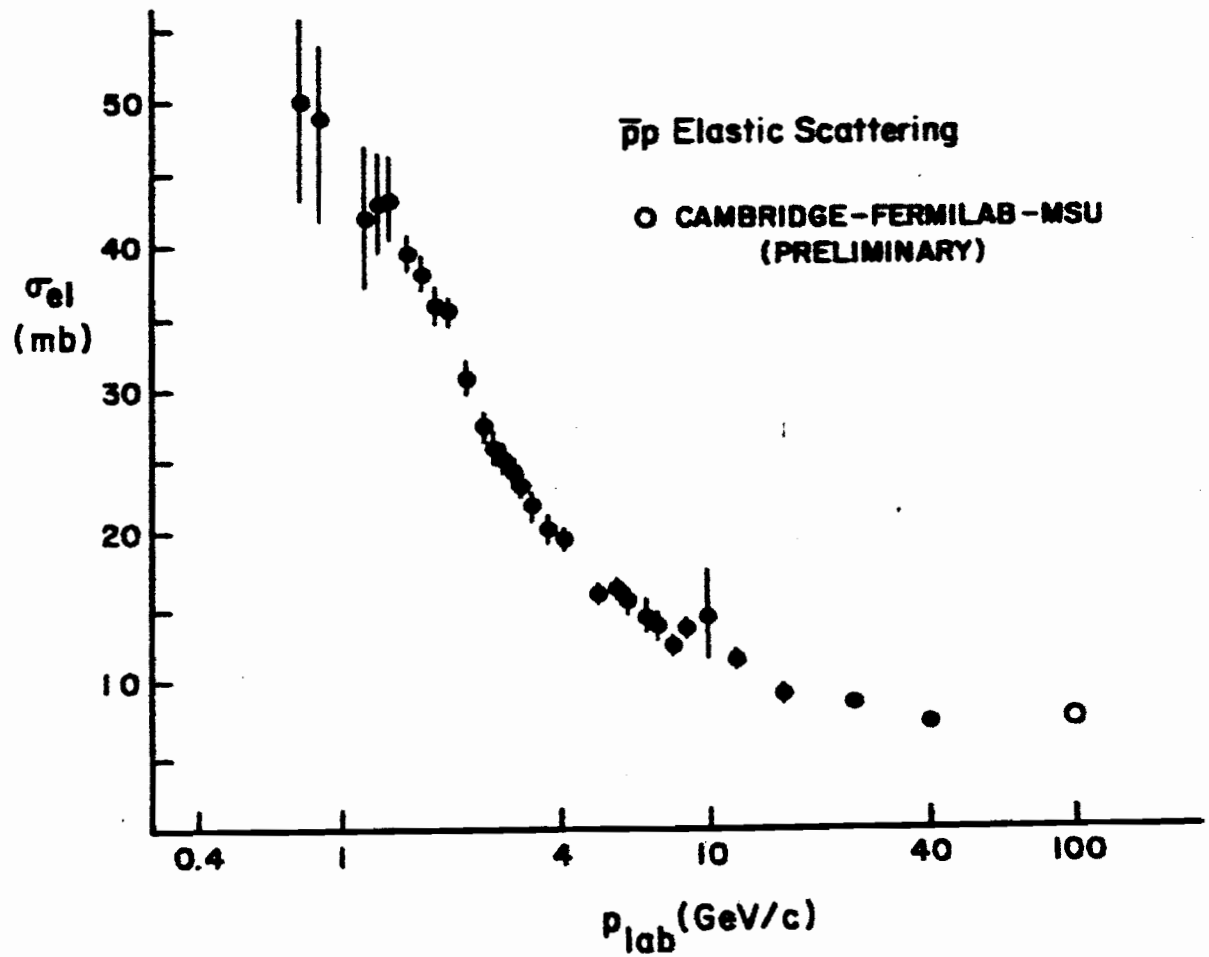

Fig. 3. $\bar{p}p$ elastic cross section as a function of the incident $\bar{p}$ momentum.

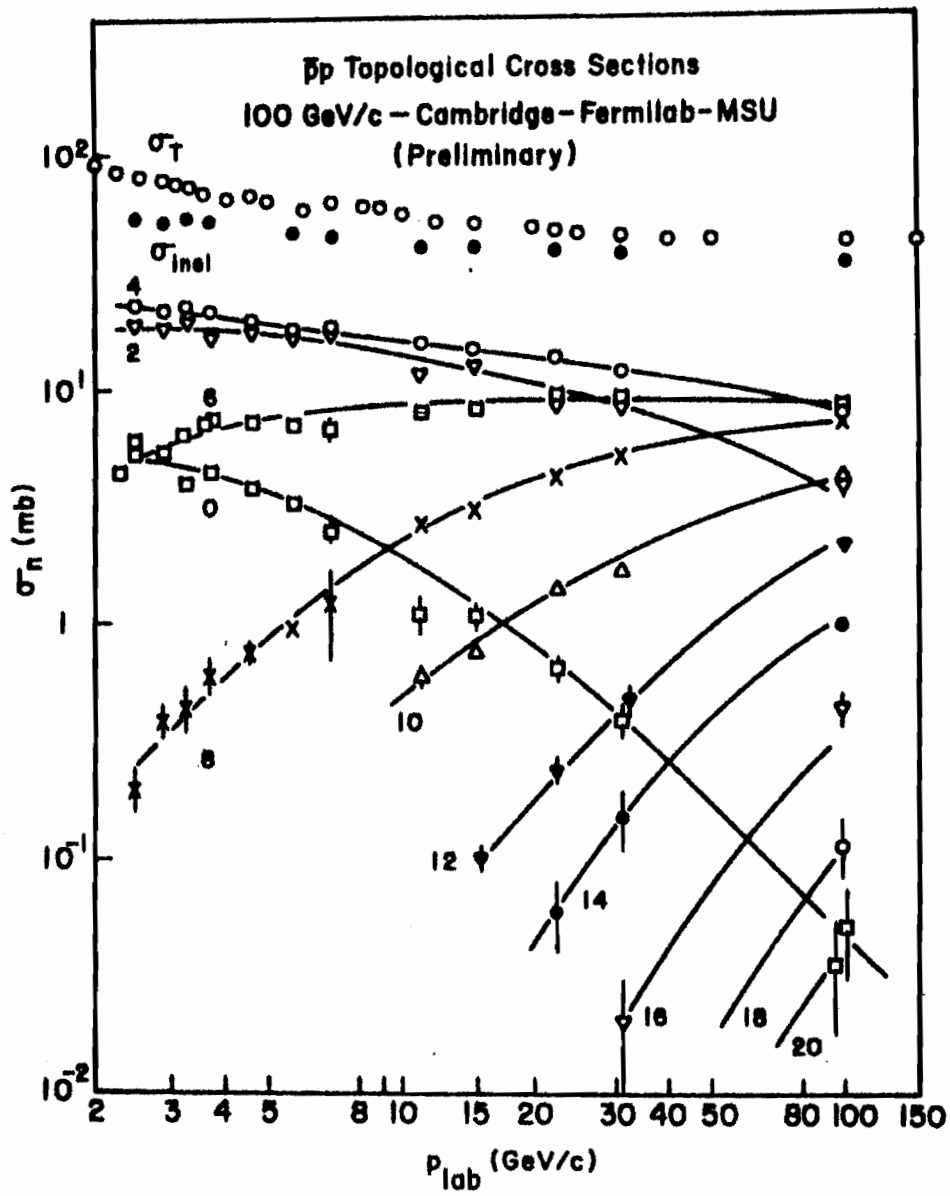

Fig. 4. Topological cross sections in $\bar{p}p$ interactions as a function of the incident $\bar{p}$ momentum.

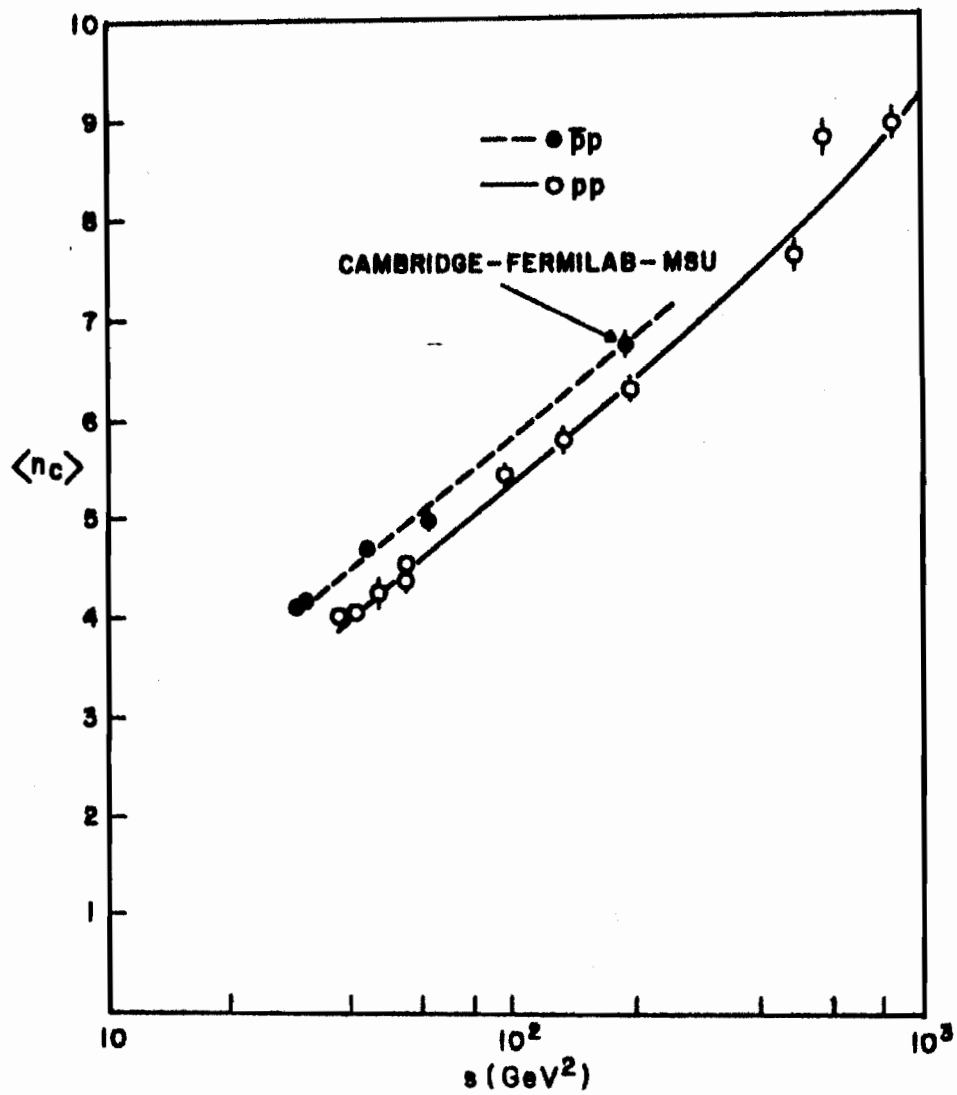

Fig. 5. Average charged particle multiplicity in $\bar{p}p$ (dashed curve) and pp (solid curve) interactions as a function of the square of the cm energy.

data with the corresponding data obtained from pp interactions. The pp data are shown as the solid curve in Figure 5 and show that at any energy the pp charged multiplicity is less than the $\bar{p}p$ multiplicity.

In Figure 6 we show the ratio of the average multiplicity to dispersion, $D = [\langle n_c^2\rangle - \langle n_c\rangle^2]^{1/2}$, for the $\bar{p}p$ and pp charge multiplicity distribution. As is well-known, the high energy pp data seem to approach a constant value of $\langle n_c\rangle/D \simeq 2$. We observe that the 100 GeV/c $\bar{p}p$ value is also consistent with this value and that for the $\bar{p}p$ interaction the ratio of $\langle n_c\rangle/D$ appears to be independent of beam momentum in the range ~7 to 100 GeV/c.

We now make a more detailed comparison between the 100 GeV/c $\bar{p}p$ and pp data. First we note that the pp data[5] have an average multiplicity $\langle n_c\rangle = 6.32 \pm 0.07$. To investigate this difference in more detail, we show in Figure 7 the inelastic multiplicity distribution for $\bar{p}p$ and pp at 100 GeV/c. The dominant feature is that the probability of producing a high multiplicity event ($n_c \gtrsim 10$) is greater in a $\bar{p}p$ collision than in a pp interaction. It would appear natural to expect that the dominant cause of this difference lies in the effects of the annihilation channels available to the $\bar{p}p$ interaction.

To further study the difference between a given topological cross section in $\bar{p}p$ and pp interactions we compare our data with one of the few theoretical predictions for this difference. Eylon and Harari,[6] with a simple duality-diagram model and unitary considerations, predict that

$$R_n = \frac{\sigma_n(\bar{p}p) - \sigma_n(pp)}{\sigma_n(pp)} = \beta^n s^{2\alpha_B - 2\alpha_M} - (1-\eta_1)\gamma^n, \quad (1)$$

where s is the square of the total cm energy, $\alpha_M(\alpha_B)$ is the intercept of the leading exchanged meson (baryon) trajectory, η_1 is some constant ($\eta_1 \lesssim 1$), and $\beta(>1)$ and $\gamma(<1)$ are constants which, in the simple model considered,[6] are $\frac{3}{2}$ and $\frac{1}{2}$ respectively. Equation (1) then predicts that:
(a) for any energy

$$R_n \underset{n \to \infty}{\to} \beta^n \cdot \text{constant} \quad (2)$$

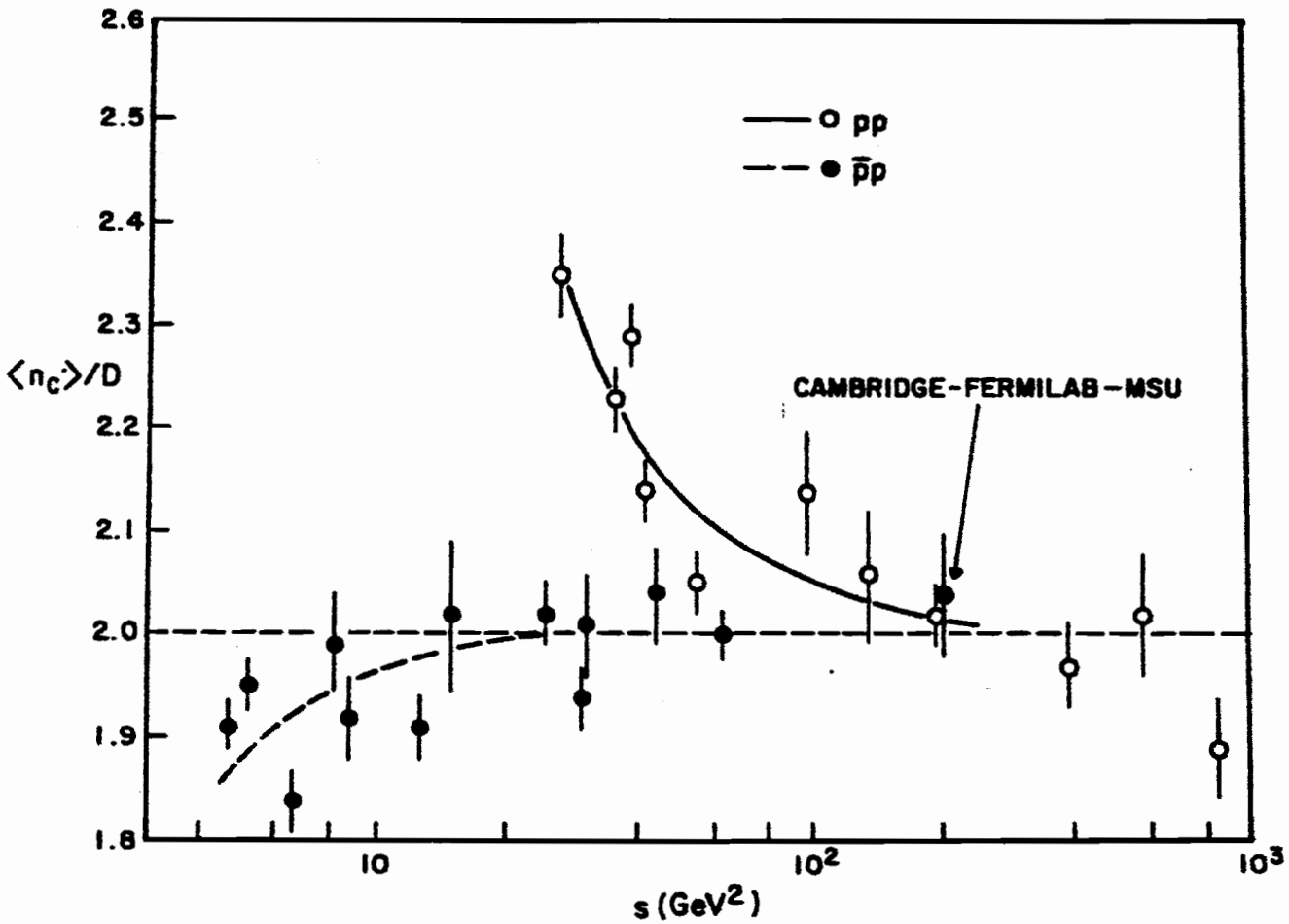

Fig. 6. Ratio of the average charged particle multiplicity to dispersion in p̄p (dashed curve) and pp (solid curve) interactions as a function of the square of the cm energy.

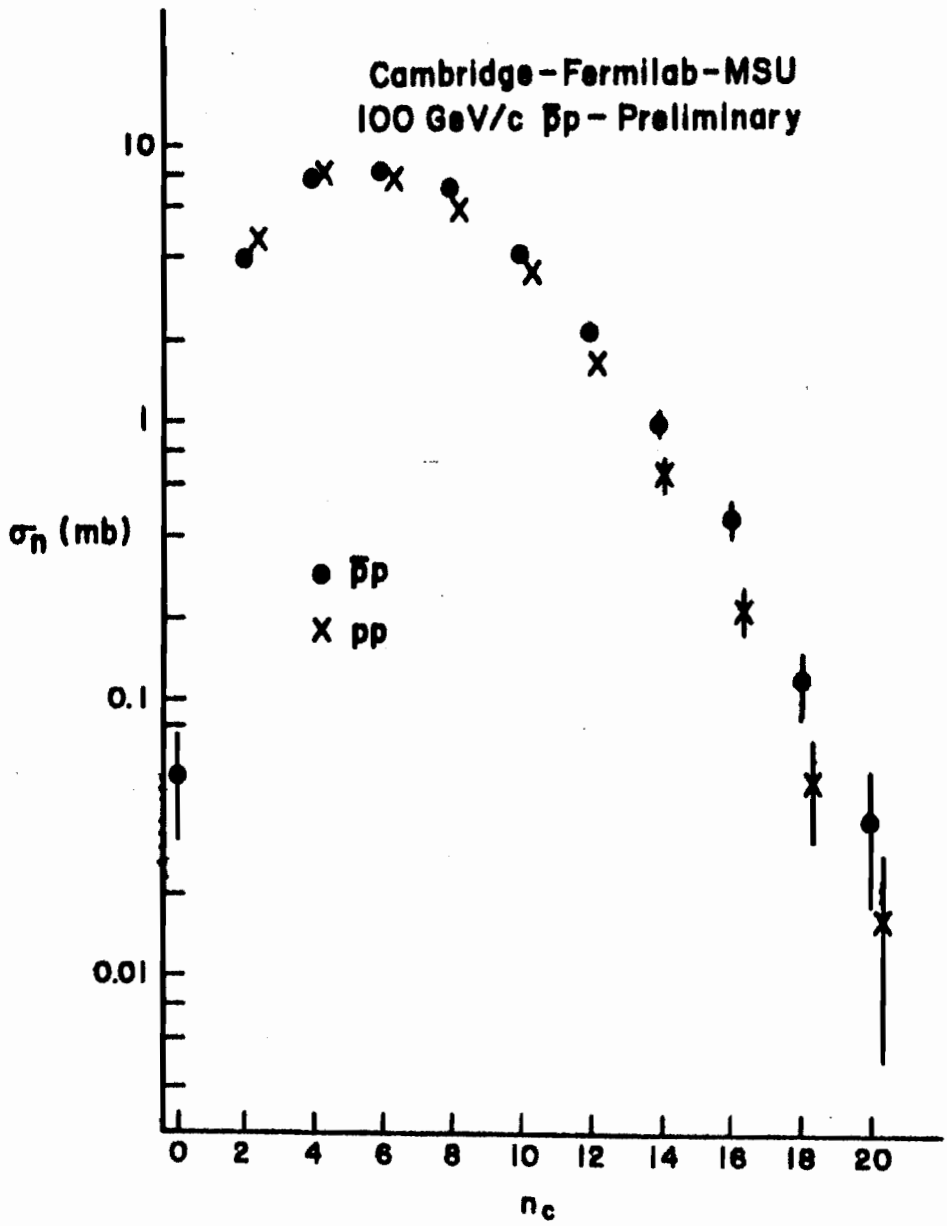

Fig. 7. Comparison of the charged particle multiplicity distributions for 100 GeV/c p̄p and pp interactions.

(b) for fixed n

$$R_n \underset{s \to \infty}{\sim} \gamma^n \text{ const,} \tag{3}$$

and (c) that the transition topology, n_t, for which $\sigma_n(\bar{p}p) = \sigma_n(pp)$ is given by $n_t = A \log s + B$, with $A = 2(\alpha_m - \alpha_B)/\log 3$ and $B = \log(1-\eta_1)/\log 3$.

To test these predictions, we can compare Fig. 4 with similar data from pp collisions[7] and note that $n_t = 2(4)$ near $s = 40(190)$ GeV^2. This implies that $(\alpha_m - \alpha_B) \simeq 0.7$ and $\eta_1 \simeq 0.94$ in reasonable agreement with the expected values. To test Eq. (3), we show in Fig. 8 R_n as a function of P_{lab} for different topologies. While R_n varies rapidly with P_{lab} it is not clear whether R_n will change sign eventually for all n. Thus it would appear that 100 GeV/c is still too low an energy to test Eq. (3).

Equation (2) is examined in Fig. 9 in which we have used $\beta = 1.25$ rather than the 3/2 suggested by Eylon and Harari. We observe that such a value does indeed give $\beta^{-n}R_n$ a constant value at 100 GeV/c but we note that it is still a poor approximation at 32 GeV/c. In conclusion it would seem that if Eq. (1) is correct then 100 GeV/c is too low an energy to make the approximations (2) and (3).

We thank the staff of the FNAL Neutrino Laboratory, M. Johnson and S. Pruss in particular, for helping to obtain the enriched beam used in this experiment. We acknowledge the conscientious work performed by our scanning and measuring personnel.

REFERENCES

* Work supported in part by the National Science Foundation, U.S.A.

** Work supported in part by the Scientific Research Council, U.K.

† Operated by the Universities Research Association, Inc., under contract with the Energy Research and Development Administration, U.S.A.

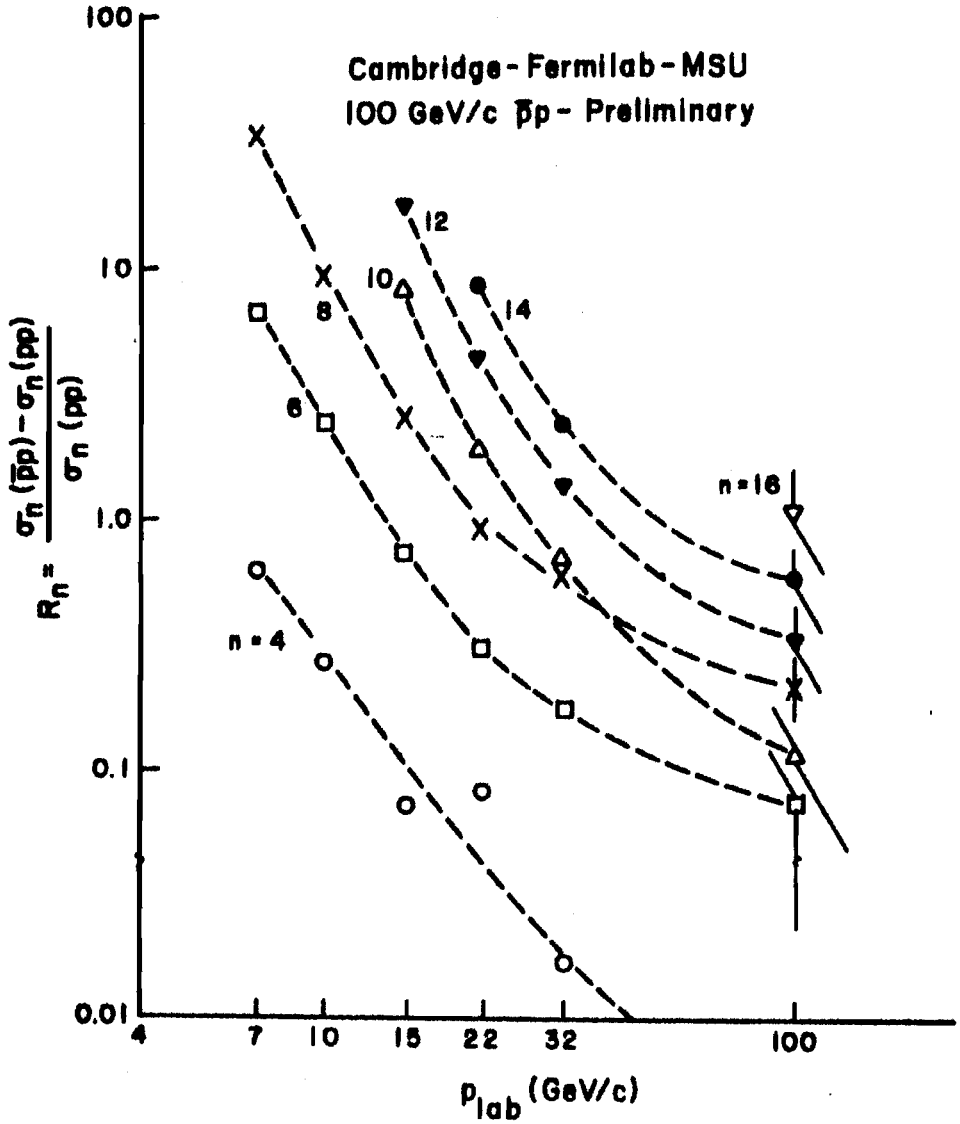

Fig. 8. The difference between p̄p and pp cross sections for a given topology as a function of the incident beam momentum.

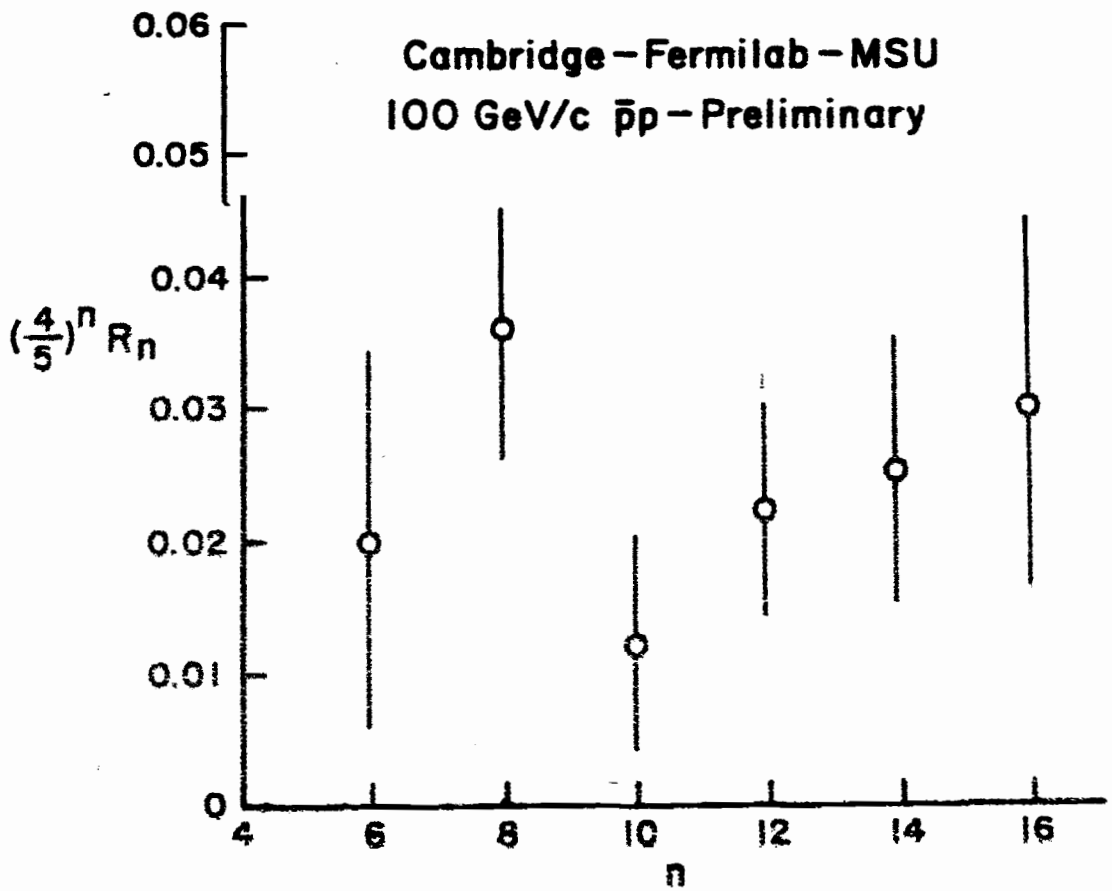

Fig. 9. The difference between p̄p and pp cross sections for a given topology at 100 GeV/c as a function of the charged particle multiplicity.

1. W. W. Neale, "Enriched Particle Beams for the Bubble Chambers at FNAL", FN-259 (1974).

2. J. Erwin et al., Phys. Rev. Letters 32, 254 (1974); V. E. Barnes et al., Phys. Rev. Letters 34, 415 (1975).

3. Preliminary data from a Michigan-FNAL-ANL-Indiana experiment (C. Akerlof et al.), summarized by J. Lach at this conference.

4. A. S. Carroll et al., Phys. Rev. Letters 33, 928 (1974).

5. C. Bromberg et al., Phys. Rev. Letters 31, 1563 (1973).

6. Y. Eylon and H. Harari, Nucl. Phys. B80, 349 (1974).

7. J. Whitmore, Phys. Rep. 10C, 273 (1974).

Table I

Topological Cross Sections for 100 GeV/c $\bar{p}p$ Interactions
Cambridge-Fermilab-MSU
(Preliminary Results)

Prong Number	Number observed	Corrected number	Cross-section (mb)	102 GeV/c pp[b]
0	6	6	0.053 ± .022	
2	el. 498	829	7.39 ± .31	7.0 ± .4
	inel. 431	443	3.95 ± .36	4.5 ± .4
4	856	869	7.75 ± .24	7.9 ± .3
6	905	906	8.08 ± .24	7.5 ± .3
8	796	790	7.05 ± .23	5.8 ± .2
10	468	461	4.11 ± .18	3.7 ± .2
12	242	235	2.10 ± .13	1.6 ± .1
14	113	109	0.972 ± .090	0.62± .07
16	51	49	0.437 ± .061	0.21± .04
18	14	13	0.115 ± .031	0.05± .02
20	4	4	0.036 ± .018	0.016±.011
Total inelastic		3885	34.65 ± .23	31.9 ± 0.7
Total	4384	4714	42.04 ± .09[a]	38.9 ± .8

[a]Reference 4.

[b]Reference 5.

Table II

Moments of Charged Multiplicity Distribution
from 100 GeV/c $\bar{p}p$ Interactions
Cambridge-Fermilab-MSU

(Preliminary Results)

	Value	102 GeV/c pp[a]
$\langle n_c \rangle$	6.74 ± 0.11	6.32 ± 0.07
D	3.30 ± 0.06	3.13 ± 0.04
$\langle n_c \rangle / D$	2.04 ± 0.06	2.02 ± 0.03
f_2^{cc}	4.1 ± 0.4	3.45 ± 0.25
f_2^{--}	-0.65 ± 0.13	0.28 ± 0.07

[a] Reference 5.